Pergamon

Geochimica et Cosmochimica Acta, Vol. 68, No. 16, pp. 3317–3325, 2004

0016-7037/04 $30.00 + .00

doi:10.1016/j.gca.2004.02.004

Transient dissolution patterns on stressed crystal surfaces

Daniel Koehn,*,† Dag Kristian Dysthe, and Bjørn Jamtveit
Physics of Geological Processes, Postbox 1048 Blindern, N-0316 Oslo, Norway

(*Received February* 13, 2003; *accepted in revised form February* 2, 2004)

Abstract—We present an experimental investigation on the dissolution of uniaxially stressed crystals of $NaClO_3$ in contact with brine. The crystals are immersed in a saturated fluid, stressed vertically by a piston and monitored constantly in situ with a CCD camera. The experiments are temperature-controlled and uniaxial shortening of the sample is measured with a high-resolution capacitance analyzer. Once the crystal is stressed it develops dissolution grooves on its free surface. The grooves are oriented with their long axis perpendicular to the direction of compressive stress and the initial distance between the parallel grooves is in accordance with the Asaro-Tiller-Grinfeld instability. We observe a novel, transient evolution of this roughness: The grooves on the crystal surface migrate upwards (against gravity), grow in size and the inter-groove distance increases linearly with time. During the coarsening of the pattern this switches from a one-dimensional geometry of parallel grooves to a two-dimensional geometry with horizontal and vertical grooves. At the end of the experiment one large groove travels across the crystal and the surface becomes smooth again. Uniaxial shortening of the crystal by pressure solution creep decays exponentially with time and shows no long term creep within the range of the resolution of the capacitance analyzer (accuracy of 100nm over a period of 14 days). This indicates that, while active, the fast transient processes on the free surface increase the solution concentration and thereby significantly slow down or stop pressure solution at the top of the crystal. This novel feedback mechanism can explain earlier results of cyclic pressure solution creep and demands development of a more complex theory of pressure-solution creep including processes that act on free surfaces.

1. INTRODUCTION

Pressure-solution creep is an important deformation mechanism in the crust of the Earth since it plays a major role in the compaction of sedimentary basins and deformation in tectonic environments (Rutter, 1976; Spiers et al., 1990; Schwartz and Stöckert, 1996). This deformation mechanism involves the dissolution of material at sites of relatively high stresses, transport in the fluid and precipitation of material at sites of relatively low stresses (Renard et al., 1999). Recent research has questioned the fundamental mechanisms of this solution-mediated deformation, notably dissolution versus healing at grain contacts (Hickman and Evans, 1992), asymmetric dissolution (Gal and Nur, 1998), dynamics of dissolution in contacts (Dysthe et al., 2002b) and the importance of free-face dissolution (den Brok and Morel, 2001; den Brok et al., 2002). The emerging radical change in our understanding of pressure-solution creep is driven by new experiments and reevaluation of the fundamental theory. We will give a short theoretical background before presenting our experimental evidence of a new transient process that we will argue may affect the whole process of pressure-solution creep.

Consider an aggregate of solid grains in a fluid under stress $\Sigma - P$, where Σ is the overburden or tectonic stress and P is the fluid pressure. We can distinguish between two different reactive sites (Fig. 1): the contact between grains where there may be a confined fluid film (Weyl, 1959; Dysthe et al., 2002a) and the free surface of grains where the stressed grains are in contact with unconfined fluid. Averaged over a large volume the fluid is saturated with respect to the grain minerals. On a local scale, however there are differences in chemical potential μ at the grain surfaces due to stresses (Srolovitz, 1989):

$$\mu = \mu_0 - (\sigma_\perp - \tfrac{1}{2}\sigma_\parallel\varepsilon_\parallel - \gamma\kappa)\Omega \qquad (1)$$

where μ_0 is the reference chemical potential at the grain surface, σ is the effective stress at the grain surface perpendicular, $\perp$, and parallel, $\parallel$, to the surface, $\varepsilon_\parallel$ is the strain parallel to the surface, γ is the interfacial tension, κ the curvature of the interface and Ω the specific atomic volume. The normal stress $\sigma_\perp$ is equal to the fluid pressure at the free surface and equal to the disjoining pressure of the confined fluid film in the contact between grains (Dysthe et al., 2002a).

Gradients in chemical potential along the grain surface and between grains drive dissolution, diffusion in the fluid phase and precipitation. Older literature on pressure solution considers smooth grains and emphasizes that from a perspective of linear irreversible thermodynamics only the normal stress part, $\sigma_\perp$, of Eqn. 1 is significant (Weyl, 1959; Paterson, 1973; Rutter, 1976). However, recent experiments and theoretical work shows that surface- and elastic energy may also be important as discussed in the next two sections.

The surface energy term in Eqn. 1, $\gamma\kappa$ is negligible for smooth theoretical grains of typical sizes $>100\mu$m. However, real grains are not smooth and recent field and experimental evidences have shown that grain contacts often have "island-channel"-like structures of 0.1–10 μm (Raj and Chyung, 1981; Spiers et al., 1990, den Brok and Spiers, 1991; Gratz and Bird, 1993) and that these evolve in time (Schutjens and Spiers, 1999; Dysthe et al., 2002a). Theoretical investigations clearly

* Author to whom correspondence should be addressed (koehn@mail.uni-mainz.de).
† *Present address:* Institut für Geowissenschaften, Tectonophysics, University of Mainz, Germany

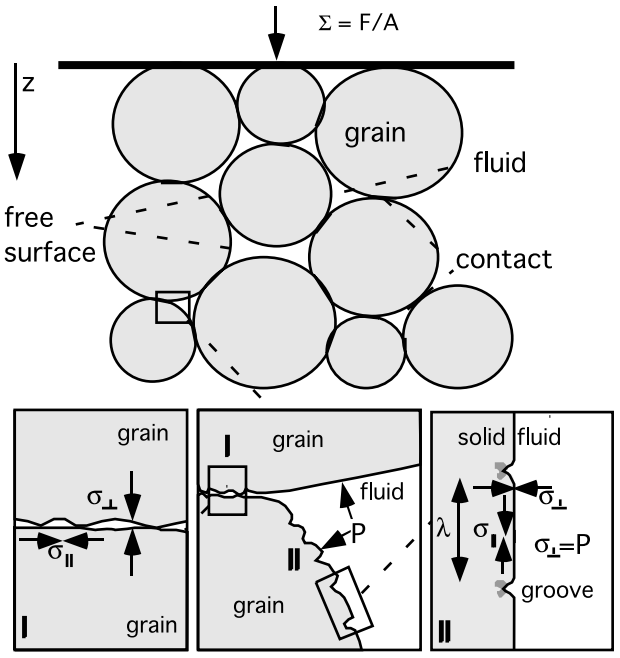

Fig. 1. Different reactive sites in an aggregate of grains under compression. The aggregate is compressed by the force F applied on the area A, which results in a stress Σ. The coordinate axis Z faces downwards. The close up in the middle shows both reactive sites. One reactive site is the contact between grains where pressure solution takes place and the other is the contact of grains to the pore fluid. P is the fluid pressure in the pores. The close up on the left hand side shows the grain-grain contact and the close up on the right hand side the open face of a grain. $\sigma_\perp$ is the stress perpendicular to the surface and $\sigma_\parallel$ the stress parallel to the surface, λ is the wavelength of the ATG-instability.

show that on this length scale the surface energy term is important (Asaro and Tiller, 1972; Yang and Srolovitz, 1993; Ghoussoub and Leroy, 2001). This term is also important in the healing of a grain contact as opposed to dissolving it (Hickman and Evans, 1992).

Also the strain energy term in Eqn. 1, $\frac{1}{2}\sigma_\parallel\varepsilon_\parallel$ seems at first glance to be negligible. However, stress localization in grooves may lead to significant amounts of strain energy. Gal and Nur (1998) showed the importance of strain energy in producing asymmetric dissolution at contacts. The strain energy term is also essential in producing stress corrosion cracking through the Asaro-Tiller-Grinfeld (ATG) instability well known in metallurgy (Asaro and Tiller, 1972; Grinfeld, 1986) and epitaxial thin film growth (Barvosa-Carter et al., 1998; Kim et al., 1999). The ATG instability is easily explained (see Fig. 1) by the strain energy concentration at the tips of grooves on the free surface of crystals. According to linear stability analysis (Srolovitz, 1989; Gal and Nur, 1998) small irregularities on the surface of a stressed crystal can grow if they are larger than a critical wavelength, λ_0. Perturbations with smaller wavelength will decay so that the crystal becomes smooth because the surface energy dominates over elastic energy. In the case of surface diffusion controlled kinetics the wavelength with the fastest growing amplitude is a factor 4/3 larger than the critical wavelength (Srolovitz, 1989):

$$\lambda_{\max} = \frac{4}{3}\lambda_0 = \frac{4\pi\gamma E}{3(\sigma_\parallel)^2}, \qquad (2)$$

where $\lambda_{\max}$ is the fastest growing wavelength, E the elastic modulus. To analyze the dynamic evolution of this instability one has to treat the full nonlinear problem (Yang and Srolovitz, 1993; Müller and Grant, 1999; Kassner et al., 2001).

Experiments on rock analog salts in *undersaturated* solution (den Brok and Morel, 2001) and on stressed aggregates (Zahid, 2001) have shown groove formation as expected from the ATG instability. However, no-one has attempted experimental or theoretical investigation of this phenomenon at fluid saturated conditions pertaining to pressure-solution creep in the Earth's crust. We have therefore performed uniaxial compression experiments on $NaClO_3$ single crystals in a saturated aqueous solution to study the dynamic interplay of the free surface instability with the $\sigma_\perp$ -driven dissolution at the contact of the crystal with the piston.

2. EXPERIMENTAL APPARATUS AND SET-UP

2.1. Experimental Apparatus

The apparatus used for the experiments is shown in Figure 2 and consists of four different parts: 1) the inner cell containing the fluid and the crystal (Fig. 2a); 2) the middle cell holding the inner cell and containing a parallel spring system to apply a force on the sample (Fig. 2b), the capacitance analyzer, two thermistors to record the temperature and a Peltier-element for precise regulation of the temperature during an experiment (Fig. 2c,d); 3) the outer cell that holds the middle cell and contains a furnace for an external temperature control (Fig. 2e); 4) and the optical system to monitor the patterns on the crystal surface in situ (Fig. 2f).

The inner cell is a standard glass cuvette with its top cut off so that it fits into the middle cell. It contains the sample crystal surrounded by brine that is covered with Hexadecane (Fig. 2a). A glass-piston with a polished contact surface is used to stress the crystal. The middle cell consists of the main apparatus that is made up of two cylindrical units that can be screwed together (see Fig. 2c,d). The lower unit contains the inner cell, two thermistors, a Peltier-element and one half of the capacitance analyzer (Fig. 2d). One thermistor measures the temperature directly at the Peltier-element and one the temperature next to the inner cell. The upper unit of the middle cell contains the friction free force system (Fig. 2c). This is made up of a micrometer-screw to apply a displacement and two sets of parallel springs, one set to hold a piston and one set to load that piston. The outer cylinder of the loading system is stationary and is connected to a moving inner cylinder by two holding springs (Fig. 2b). A micrometer-screw is used to strain a second set of springs connected to the inner cylinder and thus load the system. The applied force on the crystal is proportional to the elastic constant of the loading springs and the displacement applied by the micrometer-screw. The piston is rigidly attached to the inner cylinder of the loading system and the upper conducting plate of the capacitance analyzer. The capacitance analyzer consists of two conducting parallel plates, one on top of the lower unit and one at the bottom of the upper unit of the middle cell connected to the piston (Fig. 2c,d). If the piston is moved relative to the lower unit and the crystal, the plates of the capacitance analyzer get closer or further away from each other respectively and the capacitance (measured with an impedance analyzer) changes. With the capacitance analyzer we can measure the shortening of the crystal with a precision of 10 nm and long-term stability of 100 nm. The spring constants are chosen such that the force on the piston varies less than 1% for a shortening of 10μm. This ensures that the experiments performed are constant force experiments where the system is loaded by straining the elastic springs with the micrometer-screw. The springs themselves then apply a constant force (within 1%) on the crystal during the whole experiment.

The temperature control is assured in two stages in the same manner as in the apparatus described by Dysthe et al. (2003). Water from a

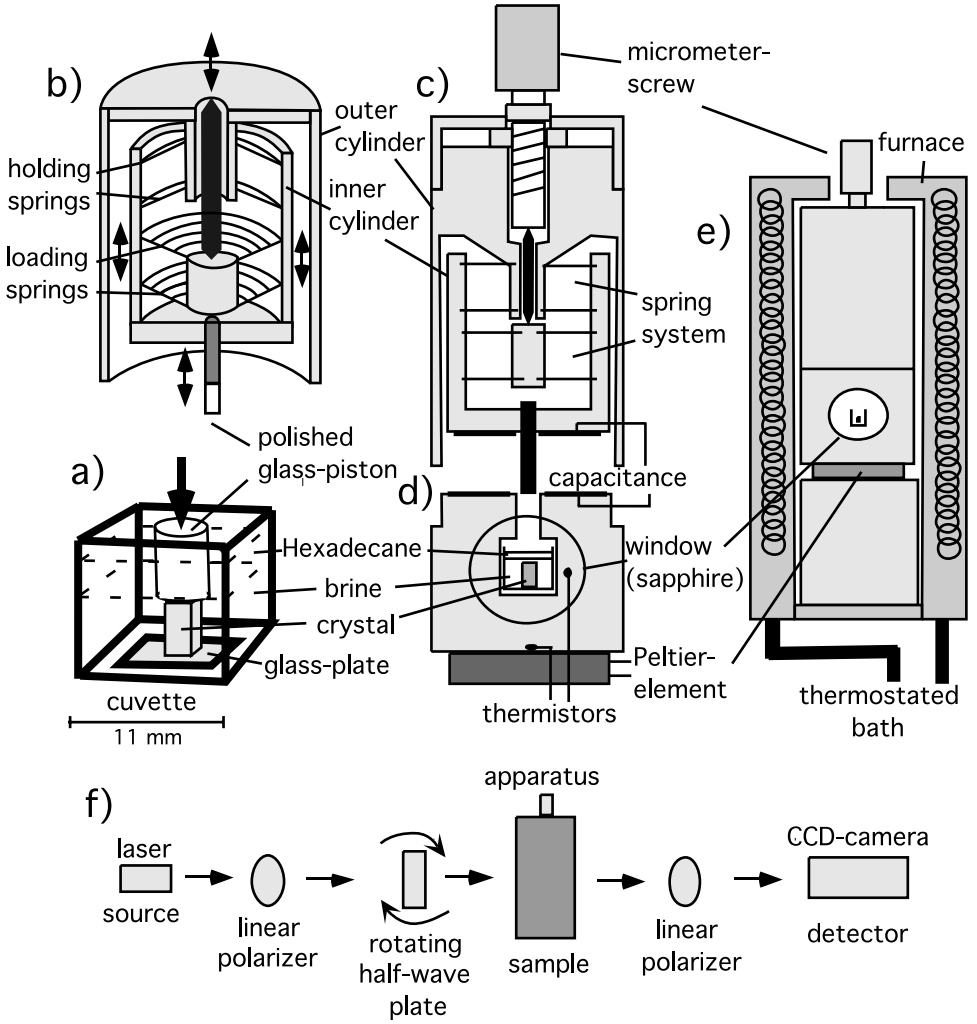

Fig. 2. Experimental apparatus and setup. a) The inner cell consists of a cuvette filled with brine and Hexadecane. The sample crystal is glued on a glass-plate and loaded with a polished glass-piston. b) The upper part of the middle cell makes up the loading system with two sets of parallel springs. An inner cylinder is fixed with two holding springs to an outer cylinder that is stationary. A second set of springs is used to load the system. c) Upper part of the middle cell with micrometer-screw, spring-system, piston and half of the capacitance analyzer. d) Lower part of the middle cell with the lower part of the capacitance analyzer, the inner cell, sapphire windows, a Peltier element and two thermistors to control temperature. The capacitance analyzer consists of two conducting plates that measure the capacitance and thus distance between the inner cylinder of the upper part of the middle cell (with the loading piston) and the lower part of the middle cell containing the sample. e) Outer part of the apparatus with the furnace for temperature control through a thermostated bath. This part of the apparatus is as well as the apparatus itself cylindrical. f) Schematic drawing showing the optical setup of the experiments. Monochromatic light from a laser source is used to illuminate the sample. Two linear polarizers and a rotating half-wave plate are used to produce and analyze polarized light and a CCD-camera is used as detector.

thermostated bath is circulated through the outer shell of the apparatus (Fig. 2e). This shell has good thermal contact with the bottom part of the middle cell. The heat flow between the outer shell and the inner cell containing the crystal and solution passes through a Peltier element. The design is symmetric to avoid gradients in temperature. The temperature measured by the thermistor at the Peltier element is used as input to a feedback control of the temperature in the inner cell (Johansen et al., 1986). The temperature that was measured 1mm from the inner cell is kept constant with a standard deviation of 0.001°C. Because there are windows in the system (Fig. 2d,e) there will be heat loss that we have not yet characterized. We estimate that this will increase the temperature fluctuation inside the sample cell by no more than a factor of ten.

Finally, we use a Charge Coupled Device (CCD) camera (Photometrix CH250) with 12bit dynamic range and 1200 × 2000 pixels spatial resolution to monitor the experiment in situ. The camera takes a picture every 30 to 240 min depending on the desired resolution in time. The crystal is illuminated by a collimated beam of transmitted light, using a laser source, two linear polarizers and a rotating half-wave plate (Fig. 2f). Surface irregularities refract the transmitted light causing bright and dark fields in the image. By analyzing the image the position of grooves on the crystal surface can be identified, but the amplitude of the roughness perpendicular to the surface cannot be measured quantitatively. To obtain this information as well we are planning experiments with white light interferometer and atomic force microscope.

2.2. Experimental Setup

In the inner cell we place a 3 to 4 mm high, 2 to 3 mm wide and 2 mm thick crystal of $NaClO_3$. We use this salt because it reacts very fast

so that the time scales of the processes are short and because at the conditions investigated it behaves elastic and brittle so that we can eliminate any effects of plasticity. The crystals were grown slowly out of a solution at the University of Oslo resulting in crystals with almost only facets on {100}. We glue the bottom of the crystal to a small glass plate to have a crystal that stands upright (Fig. 2a). After lowering the crystal into the cuvette we fill the cuvette with distilled water saturated with $NaClO_3$ at room temperature and cover the water with hexadecane to seal the cell and prevent evaporation.

We present three different experiments (More experiments at the same conditions with slight changes in crystal shape and with no glue have been performed giving consistent results with the presented experiments). All experiments are performed with $NaClO_3$ crystals of height 3–4mm, width 2–3mm and thickness 2mm in a saturated solution of $NaClO_3$ at room temperature, 22 $\pm$ 00.1°C, to minimize heat loss through the windows. Experiment one takes place at the highest stress of $\sim$8 MPa with a crystal that has two notches on the sides. Experiment two takes place at a lower stress of $\sim$4 MPa and experiment three takes place without stress. Experiments one and two are constant force experiments where a displacement is applied with the micrometer-screw to strain the elastic springs in the apparatus, which then apply a force on the crystal. We calibrated the spring system in advance to be able to calculate the force and thus the stress applied on the top of the crystal. The experiments take one to two weeks. Images showing the evolution of the surface structures are presented in Figure 3. Because the structures discussed are difficult to see in print the main features of the evolution in the three experiments have been summarized in Figure 4.

3. EXPERIMENTS

3.1. High Stress Experiment

During experiment one, pictures were taken every 2.5 h for the first 50 h and every 4.5 h for the rest, the whole experiment ran for 306.5 h. The evolution of the surface structures is illustrated in Figure 3. In the experiment we lower the crystal in the saturated solution and leave it unstressed for 24 h so that it is in equilibrium with the fluid. During these first 24 h we can observe minor smoothening of the edges of the crystal. This effect (due to surface tension) has a relatively short time-scale of 30 min to 2 h. After the first two hours the crystal surface does not change significantly. No detectable, "systematic" roughness is observed on the crystal surface.

After 24 h (time 0.0h in Fig. 3) the crystal is loaded vertically with 8 $\pm$ 00.5 MPa where upon surface patterns start to evolve. The evolution of patterns on the crystal surface takes place in three different stages. 1) The onset of an instability with the first development of mostly parallel and horizontal grooves on the crystal surface. 2) Upwards travel of grooves on the crystal surface and coarsening of the pattern. 3) One large groove travels upwards across the crystal surface leaving the surface flat again.

3.1.1. Onset of instability

Grooves on the crystal surface appear within the first 2.5 h of the experiment (see Fig. 3b). The grooves run mostly perpendicular to the principal stress direction and parallel to each other but show some braided geometries where grooves divert and rejoin. The average distance between centers of grooves is $\sim$50μm. The formation of these grooves is well explained as the onset of the ATG instability: Stress concentration at the tips of microscopic imperfections in the crystal surface drives dissolution and thereby the formation of grooves perpendicular to the principal stress (Asaro and Tiller, 1972; Grinfeld, 1986). The distance between the grooves depends on the stress and material properties.

Using Eqn. 2 we can estimate the critical wavelength from linear stability analysis of the ATG instability. The surface energy is estimated using the empirical correlation of Nielsen and Söhnel (1971) with a solubility of 9.4mol/L (Ristic et al., 1993): $\gamma = 0.012 \pm 00.01\ Jm^{-2}$, and the elastic modulus is $E=49GPa$ (Viswanathan, 1966). The fastest growing wavelength is then 38 $\pm$ 32μm. The observed wavelength of 50 μm at the onset of the instability is thus in agreement with the mean value of the theoretical prediction of 38 μm. Note that the large error in the theoretical prediction of the wavelength ($\pm$32 μm) arises from uncertainties in γ.

Around the notch on the right hand side of the crystal the grooves are not very regular and develop rhomb shapes (Fig. 3b–g), which indicates stress concentrations at the notch. Stress concentration at the notch on the right hand side deflects the direction of the maximum compressive stress towards the notch and grooves tend to develop circular shapes around the notch. This produces a rhomb pattern of grooves in the proximity of that notch and also a slight curvature of the parallel grooves towards the lower right hand corner of the crystal. One also observes that the lower right hand corner of the crystal is flat without grooves. This might be the result of a stress shadow below the notch that will prevent development of grooves.

3.1.2. Travel and coarsening of grooves

After 5 h the grooves start to travel upwards against gravity (see Fig. 3 c–f). At the same time the wavelength of the roughness increases and the grooves become larger and deeper. Note that this behavior is beyond the ATG-instability, which can only be applied to the initial development of the grooves. The coarsening of the roughness on the crystal surface is already evident after 5 h especially in the rhomb patterns next to the notch on the right hand side of the crystal. During this coarsening the pattern switches from mostly horizontal and parallel grooves to more rhomb-like shapes with horizontal and vertical grooves. This is probably due to the stress field not being uniaxial. Similar two-dimensional patterns have been obtained in simulations of a biaxially stressed solid in contact with its melt (Müller and Grant, 1999).

The coarsening of the wavelength of the roughness or distance between neighboring parallel grooves on the crystal surface is recorded for the first 90 h of the experiment and shown in Figure 5. During this time the pattern coarsens progressively with an increase in wavelength of 9.1 $\pm$ 00.4 μm/h. After the first 90 h of the experiment the pattern becomes too coarse to perform the same measure. We note, however that a coarsening with the same velocity would lead to the wavelength spanning the crystal (3mm) after 300 h. This fits well with the final evolution of the crystal surface (see below). The grooves also travel upwards with a velocity of $\sim$20 μm/h and they merge and disappear during the coarsening process.

Systems similar to our experiment but without diffusion in the fluid phase or gravity parallel to the main stress direction have recently been modeled with full nonlinear equations (Müller and Grant, 1999; Kassner et al., 2001). Müller and Grant (1999) show that in their model the wavelength of the surface instabilities grows with the square root of time. This is clearly not the case in our experiment where the wavelength grows linearly with time (Fig. 5). Kassner et al. (2001) modeled the same system and demonstrated that the coarsening (or imperfect period doubling) is due to stress shadowing where the deeper groove accelerates into the crystal whereas the smaller grooves get less stressed and vanish due to surface tension. In their system the grooves do not move parallel to the surface as they do in our experiments. The gravity and diffusion in our experiments thus change both the coarsening mechanism and scaling with time relative to the mentioned model (see section 4.1 in the "Discussion").

3.1.3. Superstructure

After $\sim$25 h a large "groove" starts to develop at the bottom of the crystal (see Fig. 3 f–i). We term this "groove" a superstructure after Kassner et al. (2001). The superstructure first increases its depth and width for another 20 h and then starts to move upwards. The crystal surface below the large groove has almost perfect crystal facets and the notches go from being rounded to developing straight surfaces parallel to low Miller index crystal facets when the groove has gone past. While the superstructure moves upwards it overtakes the smaller grooves that still remained on the crystal surface. Grooves that lie in front of the superstructure are not stable but break up into rhomb structures. At the end of the experiment the crystal develops an almost perfect shape with flat facets.

Figure 6 shows a plot of the velocity of the superstructure in experiment one versus time. The large groove travels upwards with a

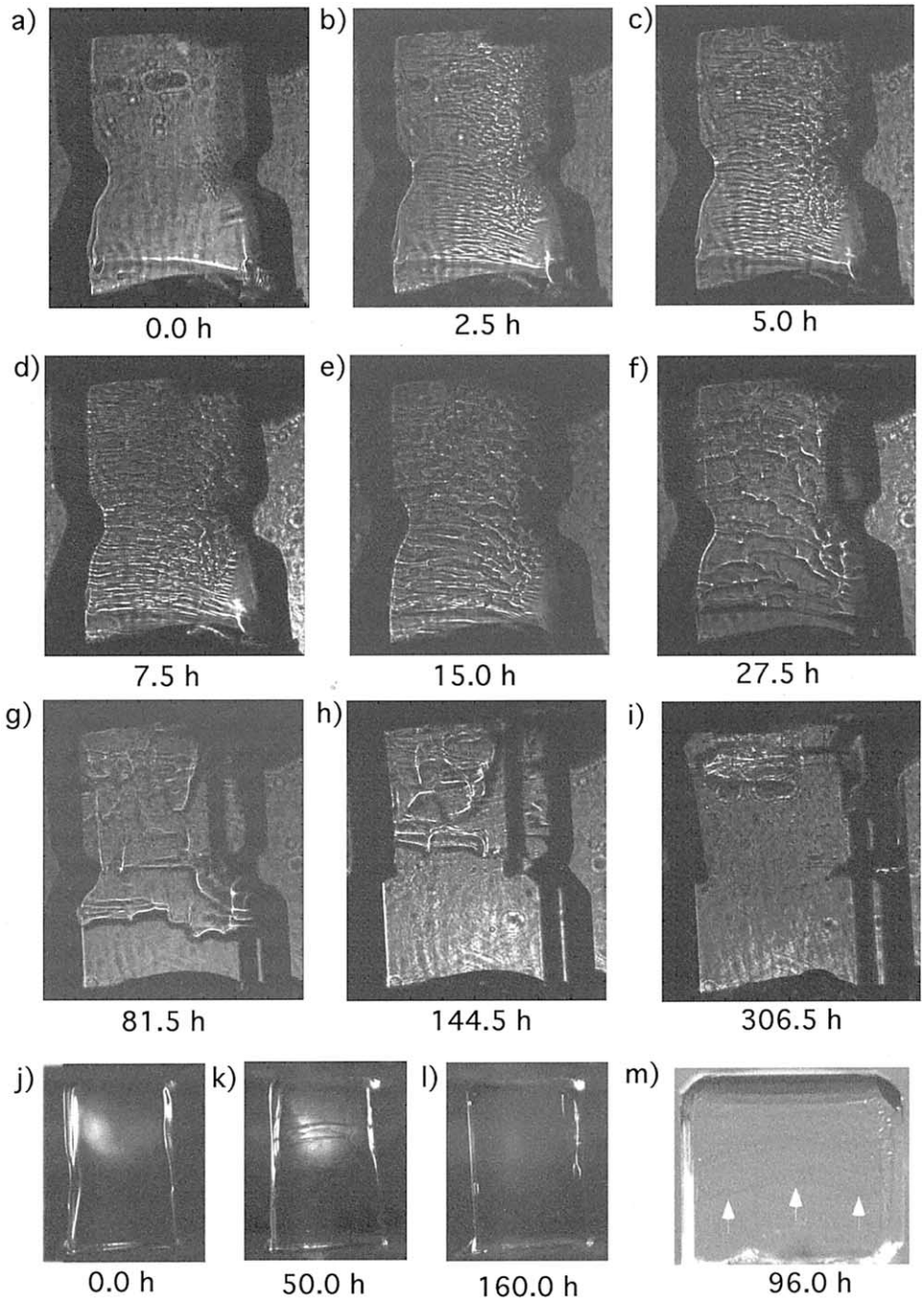

Fig. 3. Images of the crystal surface during the three experiments. Experiment one is shown in picture a to i, experiment two in picture j to l and experiment three in picture m. The height of the crystal in experiment 1 and 2 is 3mm and in experiment 3 is 4mm. The images captured at different instants show the evolution of patterns on the crystal surfaces including surface energy effects and stress effects that lead to a roughening of the surface, the coarsening of the pattern and the progress towards smooth crystal surfaces again.

mean velocity of 20μm/h. At 120 h when it crosses the notches on the crystal the groove moves 3 times faster. The sudden increase in velocity may be related to stress concentrations between the notches, however further theoretical work is needed to fully understand the traveling of grooves.

After 310 h the stress is released on the crystal and it starts to grow but keeps its faceted surfaces. Growth of the crystal after stress release indicates that the fluid is oversaturated. The crystal grows because in the stressed state the chemical potential of the crystal was increased with respect to the fluid. The crystal therefore dissolved and the $NaClO_3$ concentration in the fluid increased. This leads to an oversaturation of the fluid once the stress is released and the crystal grows. The volume of solid dissolved (and reprecipitated once the stress is released) should be proportional to the fluid volume in the experiment. However, since we only observe the crystal growth in the image plane we cannot estimate the volume change of the crystal. In future exper-

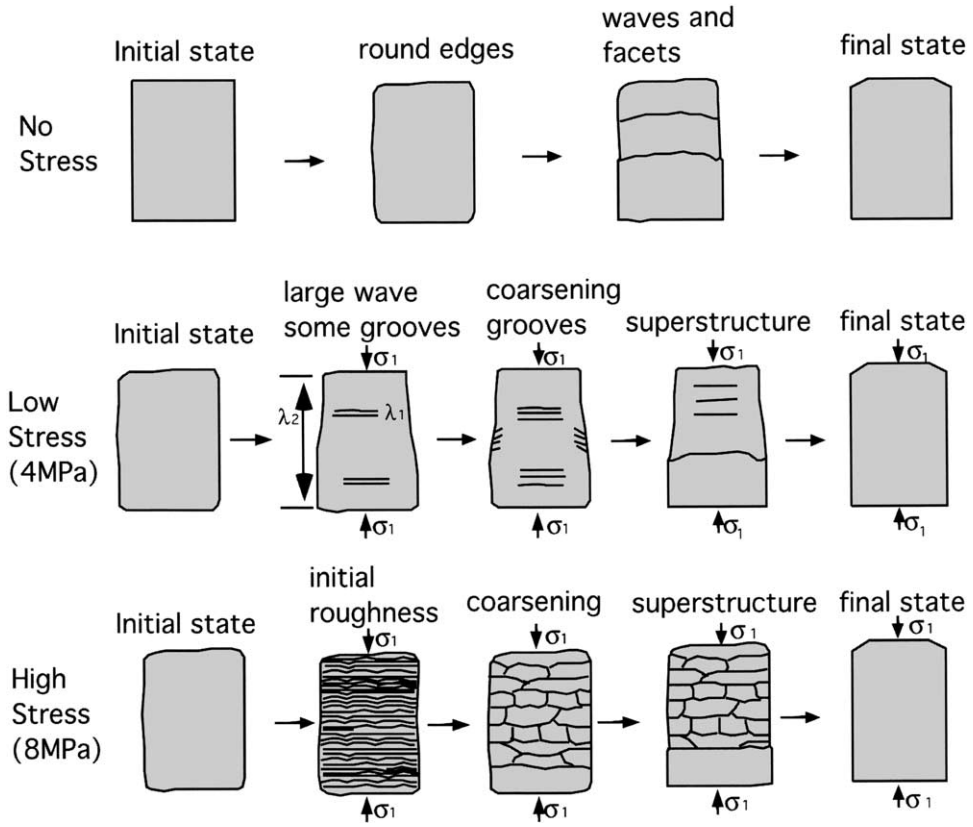

Fig. 4. Summary of transient patterns on crystals at three different stress conditions through time. The first row shows the effects of the surface energy. The second and third row show coupled surface energy and stress effects. The surface develops a roughness that goes through a coarsening, develops a superstructure and becomes flat again.

iments we will attempt to measure the solution concentration in situ by interferometry.

3.1.4. Shortening by pressure solution creep

Figure 7 shows the vertical shortening of the crystal versus time as measured with the capacitance analyzer during experiment one. The first 6 h the crystal is shortened by pressure solution creep at the contact to the piston. The creep decays exponentially with time with a time constant of ~1h. The exponential decay is unexpected because according to ordinary theory of pressure solution creep (Rutter, 1976) the shortening should after a short time reach a steady state velocity, not decay to zero velocity. At ~6 h there is a jump of 7 μm in the crystal height, which is probably due to crushing of a small contact. This jump reinitiates the decay rate (such re-initiation has been thoroughly documented for NaCl, Dysthe et al., 2003) that again decays exponentially with a time constant of 1h. Note that the jump does not change the force

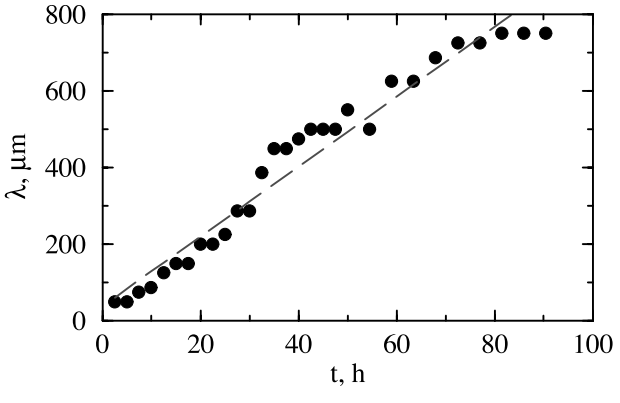

Fig. 5. Distance, λ between neighboring parallel grooves or wavelength of the roughness versus time. The wavelength increases during the experiment, which indicates that the pattern coarsens. The coarsening is linear within the first 90 h of the experiment with a velocity of ~9.1 ± 00.4 μm/h.

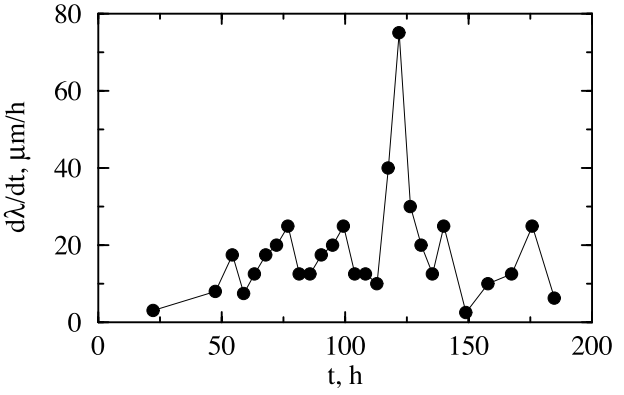

Fig. 6. Velocity of the movement of the superstructure in experiment 1 across the crystal against time. The mean velocity is 20μm/h. Note that the groove accelerates once it crosses the two notches.

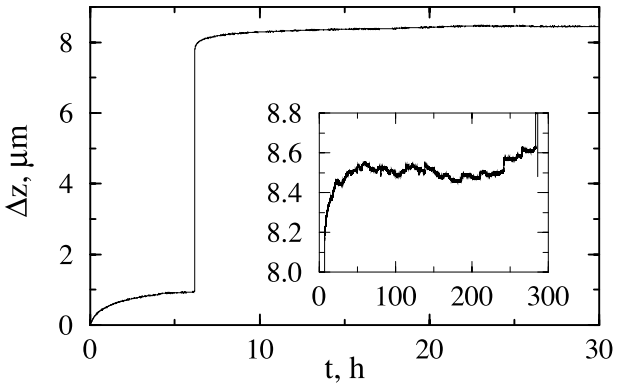

Fig. 7. Vertical shortening versus time for as measured with the capacitance analyzer during experiment one. The first 6 h the crystal is shortened by pressure solution creep. The creep decays exponentially with a time constant of ~1h. Then there is a jump of 7μm in the crystal height, probably due to crushing of a small contact. This jump reinitiates the decay rate that again decays exponentially with a time constant of 1h. The inset shows that there is no long time creep, the crystal is not shortening due to pressure solution at the contact to the piston within the timescale of the experiment (300 h). The fluctuations have a standard deviation of 20nm.

applied by the piston. For the last 250 h we observe no more creep with the high-resolution analyzer (resolution of 100nm).

3.2. Low Stress Experiment

In experiment two we use a crystal without notches and reduce the stress to 4MPa. As can be seen from Figure 3 j–l the general evolution of patterns in experiment one and two are similar. Once the crystal is stressed it develops a roughness, grooves travel upwards and coarsen until a superstructure runs across the crystal and it becomes flat again. Since the crystal in experiment two contains no notches it can develop perfect crystal facets on its front and sides. Similar to experiment one the crystal develops edges on its upper surface towards the piston that have an orientation of ~45° relative to the top and sides. The main difference of the pattern in experiment one to experiment two is that in experiment two grooves on the crystal surface are not as pronounced as in experiment one and start out with a larger wavelength. The crystal seems to develop two different wavelengths at the same time (see Fig. 4). The shorter wavelength (λ_1): small grooves on the crystal surface with an initial wavelength of 180 μm. The grooves travel upwards with a velocity of 20 μm/h and go through a similar coarsening as in experiment one. The second wavelength (λ_2) seems to be as large as the crystal so that the upper part of the crystal dissolves and forms the valley of the wave and the lower part of the crystal forms the hill. This wave merges with the superstructure after 50 h and then travels upwards with a maximum velocity of ~20 μm/h.

The initial, smaller wavelength of 180 μm is in good agreement with the fastest growing wavelength $\lambda_{max} = 150 \pm 130$ μm from Eqn. 2. The grooves in experiment two develop later than the grooves in experiment one. This result is also in agreement with linear stability analysis that indicates that grooves on the surface of higher stressed crystals will grow faster and thus can develop earlier in the experiment (Srolovitz, 1989; Gal and Nur, 1998).

3.3. Experiment with No Stress

Experiment three was performed with no stress on the crystal. In this experiment we wanted to study possible long-term effects of the surface energy. In experiment three we observe the same short-term effects as in the other two experiments. The surface energy will smoothen the edges of the crystal relatively fast within tens of minutes to hours. However after a few days we observe that small waves or growth-fronts travel upwards on the crystal until it develops crystal facets. These small waves corresponding to the formation of the superstructure in the other two experiments must be a long-term effect of the surface energy on the crystal. Note that the waves or growth-fronts on the unstressed crystal are very small compared to the stress-induced grooves (1:5 to 1:100).

4. DISCUSSION

4.1. Traveling and Coarsening of Grooves

The persistent traveling of grooves upwards along the surface of the crystals while the distance between surviving grooves increases (coarsening) is a phenomenon that, to our knowledge, has not been reported before. den Brok et al. (2002) did observe grooves moving freely on the surface of a stressed K-alum crystal. They used an undersaturated solution and they did not observe persistent coarsening. Therefore they termed the grooves dynamically stable. From nonlinear simulations of similar systems, however it is expected that the structure coarsens: The stress concentration at the deepest groove tip will relieve the stress at neighboring, shallower grooves and thus cause a coarsening.

There are two important differences between our observations and predictions from modeling. We observe traveling grooves, not stationary grooves that become deeper or vanish and we observe a different time dependence of the coarsening.

As already mentioned the difference between our experiments and simulations based on the nonlinear equations of the ATG instability (Müller and Grant, 1999; Kassner et al., 2001) is the gravity along the principal stress direction and diffusion of dissolved material in the fluid phase. During the initial development of the ATG instability diffusion is not important in our experiments as long as the fluid is undersaturated (once the crystal is stressed). However, traveling of grooves and coarsening of the patterns involve diffusion of material in the fluid, for example from the upper edge of a traveling groove towards its lower edge. The gravity breaks the symmetry and introduces a direction in the experiments and diffusion introduces a new time scale. The new time scale introduced by the fluid phase diffusion may explain the growth of the wavelength proportional to time as opposed to proportional to square root of time in the simulations of Müller and Grant (1999) who modelled a solid in contact with its melt where no diffusion takes place.

The traveling of grooves is probably due to concentration gradients in the fluid that develop as an effect of gravity (possibly enhanced by convection) causing higher concentration (and density) at the bottom of the cell. The upper edge of a groove on the crystal surface will therefore tend to dissolve and the lower edge will tend to grow (see Fig. 8). This effect will result in a traveling of grooves along the concentration gradient in the fluid towards the top of the crystal. Concentration gradients in the fluid can also explain the small traveling waves or growth fronts on the unstressed crystal. The unstressed crystal is initially in equilibrium with the fluid but is in local disequilibrium once concentration gradients develop. We are currently working on modeling the experimental system to evaluate these effects quantitatively.

4.2. Superstructure and Phase-Transition

In all three experiments one can observe short-term surface energy effects that round the crystal edges and long-term sur-

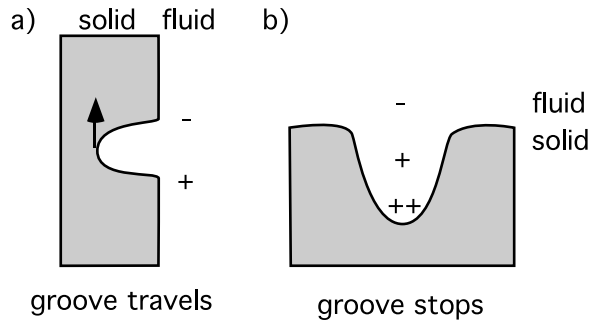

Fig. 8. How different orientations of grooves relative to a concentration gradient in the fluid produce different behavior. In case a) the concentration gradient induces an upward velocity and in case b) it stops the amplitude growth of the groove.

face energy effects (probably induced by concentration gradients in the fluid) where waves or growth fronts travel up the crystal and the crystal becomes flat. These surface energy effects interact with the stress-induced roughness in two ways. The initial rounding of edges of the crystal may help to induce the ATG-instability since it is harder to break perfect crystal facets. The long-term effect of the surface energy seems to couple with the stress induced grooves once the roughness has coarsened up to the same scale as the surface energy waves. This scale is probably identical to or in the same range as the height of the crystal. The system then develops the so termed superstructure that is most pronounced in experiment one. Below this large groove the surface energy produces perfect crystal facets. No new grooves will develop below the superstructure because the wavelength of the roughness is larger than the crystal. After the crystal has developed a flat shape it has reached a new equilibrium under stress and no new grooves will develop. No gradients in elastic- or surface energy exist along the flat surface, which makes the crystal very stable. This new, stable phase of the crystal demands a thorough, theoretical explanation, we will only discuss it in qualitative terms.

The developing patterns on the crystal surface seem to be a transition towards a new equilibrium of the system under stress. The patterns are more pronounced if the system is driven further out of equilibrium i.e., if the stress on the crystal is higher. The transition of the rough crystal surface to a smooth one is similar to a first order phase transition. This is also supported by the observation that the stressed crystal does not develop new patterns (like grooves) when the stress is released; it grows but remains smooth. The stress-roughening process is not easily reversible which is typical for first order phase transitions.

The stability of the new, flat crystal surface suggests that it is in equilibrium with the fluid. One possibility is that a new, solid unstrained layer without stresses has grown on the crystal. Such an unstrained layer will evidently be in equilibrium with a saturated solution. The other possibility is that the fluid becomes supersaturated by the stressed crystal. This is supported by the fact that the crystal grows significantly once the stress is removed and by the slowing down of the pressure solution. It remains to be shown, however, that a bulk liquid can be driven into a thermodynamically unstable state by such a surface process. We are therefore planning to measure the solution concentration in situ by interferometry during the experiments.

4.3. Coupling to Pressure Solution Creep

Another important question concerns the comparability of our experiments to compacting aggregates of grains in common rock-forming systems. Will an aggregate of calcite or quartz grains behave in a similar way as the single crystals of $NaClO_3$ in our experiments? The main differences between our experimental setup and a natural system (for example a porous sandstone) are that we have a larger fluid volume and that our system is loaded suddenly. Especially the sudden input of energy may trigger the ATG instability. However natural systems may also go through sudden changes of stresses for example during earthquake or fault movement. In compacting systems without change in external stress one expects rearrangement of the local stress network in the aggregate due to grain sliding. Experiments in progress show such measurable, sudden changes in stress during compaction. This will probably be sufficient to trigger instabilities both at free surfaces and in contacts (Dysthe et al., 2003). Transient processes acting on free surfaces may be very important in these cases.

From the capacitance curve in Figure 7 one can observe that in experiment one the shortening of the crystal after 20 h is of the order 0.5 nm/h (strain rate of 3.8×10^{-11} s−1) after a period of transient creep. Dysthe et al. (2002b) measured pressure solution creep rates of NaCl at 4MPa and 20 °C to be 170 nm/h after 10 h. Because $NaClO_3$ is more soluble and the stress used here is larger one would expect the rate of shortening of $NaClO_3$ to be almost 3 orders of magnitude larger. Dysthe et al. (2002b) also showed that for NaCl the transient creep can be related to a structural change of the contact surface in an experiment where an indentor is pushed onto a crystal surface. In a similar manner to the transient free surface structures in our experiments the confined surface of the NaCl-crystals evolves from a rough island-channel geometry towards a smooth surface. Stress and temperature fluctuations can reinitiate the structural change and thus the period of transient creep (Dysthe et al., 2003), which probably happened in our experiments after the sudden jump in the capacitance curve (Fig. 7). The processes that take place on the free surface of the crystal are obviously faster and more important than pressure solution at the contact of the piston to the crystal. This observation does not easily fit into existing models of pressure solution where the crystal is supposed to dissolve at the contact with the piston and precipitate on the sides. In our experiment pressure solution at the piston is either very slow compared to processes on the surface or is slowed down or even stopped by the processes on the surface. Both processes can interact through the fluid. The processes at the free surface are faster because the diffusion is faster in the free fluid than in the confined fluid in the contact. Our interpretation is that the fast process on the surface over-saturates the fluid at the beginning of the experiment which will temporarily stop pressure solution at the contact with the piston.

We are of the opinion that in natural systems at least in some situations, processes on free surfaces will interact with pressure solution creep at confined contacts in a manner similar to our experiments. However, further experimental studies in this area are needed.

Finally our experimental results might shed light on the experiments of Martins et al. (1999) who found cyclic behavior in compaction rates of single crystals of halite. If the system switches between processes happening on the free surface that slow down shortening and processes on the confined surface that induce shortening it might show a cyclic behavior. In that case our experiments show an extreme case where only processes on the free surface are important and the crystal stops shortening after a short period of time.

5. CONCLUSIONS

Experimental measurements on stressed crystals of $NaClO_3$ in a saturated solution have shown that transient patterns develop on the crystal surface. These structures can be subdivided into an initial roughening of the crystal surface, a coarsening process and a phase-transition towards a flat surface. The initial roughness is made up of parallel grooves perpendicular to the compressive stress with an initial distance from each other that is in agreement with linear stability analysis of the ATG instability. We have measured quantitatively a new mode of coarsening of the structure with the wavelength growing linearly with time and the grooves traveling upwards along the crystal surface. At the end of the coarsening event one large groove or superstructure travels along the crystal and leaves a flat faceted crystal surface behind. Slow surface energy waves on the crystal and the grooves due to stress are coupled together once they reach a common wavelength and form the superstructure. The pressure solution creep at the contact of the crystal to the piston slows down to below 0.5 nm/h, which is the accuracy of the high-resolution capacitance analyzer used. We argue that this is the result of the transient processes at the free surface that increase the solution concentration. This novel feedback mechanism can explain earlier results of cyclic pressure solution creep and demands the development of a more complex theory of pressure-solution creep.

Acknowledgments—The authors are grateful to Ola Nilsen for growing excellent $NaClO_3$-crystals, to Heloise Soldi-Lose for calibrating the double spring load and to Jens Feder, Renaud Toussaint and Francois Renard for valuable discussions. This project was funded by a grant from the Center of Advanced Studies at the Norwegian Academy of Sciences, by the EU-Network "Precip-Dissolution" contract number HPRN-CT-2000–00058 and by "Physics of Geological Processes" a Norwegian Center of Excellence funded by the Norwegian Research Council.

Associate editor: R. A. Wogelius

REFERENCES

Asaro R. J. and Tiller W. A. (1972) Interface morphology development during stress corrosion cracking: Part I, via surface diffusion. *Metall. Trans.* **3,** 1789–1796.

Barvosa-Carter W., Aziz M. J., Gray L. J., and Kaplan T. (1998) Kinetically driven growth instability in stressed solids. *Phys. Rev. Lett.* **81,** 1445–1448.

den Brok B. and Spiers C. J. (1991) Experimental evidence for water weakening of quartzite by microcracking plus solution precipitation creep. *J. Geol. Soc.* **148,** 541–548.

den Brok B. and Morel J. (2001) The effect of elastic strain on the microstructure of free surfaces of stressed minerals in contact with an aqueous solution. *Geophys. Res. Lett.* **28,** 603–606.

den Brok B., Morel J, Zahid M (2002) In situ experimental study of roughness development at a stressed solid/fluid interface. In *Deformation Mechanisms, Rheology and Tectonics: Current Status and Future Perspectives. Geological Society Special Publications* **vol. 200**.

Dysthe D. K., Renard F., Porcheron F., and Rousseau B. (2002a) Fluid in mineral interfaces –molecular simulations of structure and diffusion. *Geophys. Res. Lett.* **29,** 7–13.

Dysthe D. K., Podladchikov Y., Renard F., Feder J., and Jamtveit B. (2002b) Universal scaling in pressure solution creep. *Phys. Rev. Lett.* **89,** 24610.2.

Dysthe D. K., Renard F., Feder J., Jamtveit B., Meakin P., and Jøssang T. (2003) High resolution measurements of pressure solution creep. *Phys. Rev. E.* **68,** 01160.3.

Gal D. and Nur A. (1998) Elastic strain energy as a control in the evolution of asymmetric pressure-solution contacts. *Geol.* **26,** 663–665.

Grinfeld M. A. (1986) Instability of the separation boundary between a non-hydrostatically stressed solid and a melt. *Sov. Phys. Dokl.* **31,** 831.

Ghoussoub J. and Leroy Y. M. (2001) Solid-fluid phase transformation within grain boundaries during compaction by pressure solution. *J. Mech. Phys. Solids* **49,** 2385–2430.

Gratz A. J. and Bird P. (1993) Quartz dissolution: theory of rough and smooth surfaces. *Geochim. Cosmochim. Acta* **57,** 977–989.

Hickman S. H. and Evans B. (1992) Growth of grain contacts in Halite by solution-transfer: Implications for diagenesis, lithification and strength recovery. In *Fault mechanics and transport properties of rocks* Academic Press, San Diego, 253–280.

Johansen T. H., Feder J., and Jøssang T. (1986) Computer-controlled high-resolution capacitance dilatometer/oven systems: Design, instrumentation, and performance. *Rev. Sci. Instr.* **57,** 1168–1174.

Kassner K., Misbah C., Müller J., Kappey J., and Kohlert P. (2001) Phae-field modeling of stress-induced instabilities. *Phys. Rev. E.* **63,** 03611.7.

Kim K. S., Hurtado J. A., and Tan H. (1999) Evolution of a surface-roughness spectrum caused by stress in nanometer-scale chemical etching. *Phys. Rev. Lett.* **83,** 3872–3875.

Martins B., Röller K., and Stöckert B. (1999) Low-stress pressure solution experiments on halite single-crystals. *Tectonophys.* **308,** 299–310.

Müller J. and Grant M. (1999) Model of surface instabilities induced by stress. *Phys. Rev. Lett.* **82,** 1736–1739.

Nielsen A. E. and Söhnel O. (1971) Interfacial tensions of electrolyte crystals in aquaeous solution from nucleation data. *J. Cryst. Growth* **11,** 233–242.

Paterson M. S. (1973) Nonhydrostatic Thermodynamics and its geological applications. *Rev. Geophy. Space Phys.* **11,** 355–389.

Raj R. and Chyung C. K. (1981) Solution-precipitation creep in glass ceramics. *Acta Metall.* **29,** 159–166.

Renard F., Ortoleva P., and Gratier J. P. (1999) An integrated mode for transitional pressure solution in sandstones. *Tectonophys.* **312,** 97–115.

Ristic R. I., Sherwood J. N., and Wojciechowski K. (1993) Morphology and growth kinetics of large sodium chlorate crystals grown in the presence and absence of sodium dithionate impurity. *J. Phys. Chem.* **97,** 10774–10782.

Rutter E. H. (1976) The kinetics of rock deformation by pressure solution. *Phil. Trans. Royal Soc. London* **283,** 203–219.

Schutjens P. M. and Spiers C. S. (1999) Intergranular pressure solution in NaCl: Grain-to-grain contact experiments under the optical microscope. *Oil Gas Sci. Techn.* **54,** 729–750.

Schwartz S. and Stöckert B. (1996) Pressure solution in siliciclastic HP-LT metamorphic rocks- constraints on the state of stress in deep level accretionary complexes. *Tecton.* **255,** 203–209.

Spiers C. J, Schutjens P. M, Brzesowsky R. H, Peach C. J, Liezenberg J. L, Zwart H. J (1990) Experimental determination of constitutive parameters governing creep of rocksalt by pressure solution. In *Deformation Mechanisms, Rheology and Tectonics*, vol. 54, pp. 215–227. Geological Society Special Publication.

Srolovitz D. J. (1989) On the stability of surfaces of stressed solids. *Acta Metall.* **37,** 621–625.

Viswanathan R. (1966) Elastic constants of sodium chlorate single crystals by pulse-echo method. *J. Appl. Phys.* **37,** 884–888.

Weyl P. K. (1959) Pressure solution and the force of crystallization—a phenomenological theory. *J. Geophys. Res.* **69,** 2001–2025.

Yang W. H. and Srolovitz D. J. (1993) Cracklike surface instabilities in stressed solids. *Phys. Rev. Lett.* **71,** 1593–1596.

Zahid M (2001) Duktile Gesteinsdeformation durch zeitabhängige Kataklase. Doktoral Thesis, Johannes Gutenberg University, Mainz, 111.